Fission yeast TRP channel Pkd2p localizes to the cleavage furrow and regulates cell separation during cytokinesis

Zachary Morris, Debatrayee Sinha, Abhishek Poddar, Brittni Morris, and Qian Chen*
Department of Biological Sciences, University of Toledo, Toledo, OH 43606

ABSTRACT **Force plays a central role in separating daughter cells during cytokinesis, the last stage of cell division. However, the mechanism of force sensing during cytokinesis remains unknown. Here we discovered that Pkd2p, a putative force-sensing transient receptor potential channel, localizes to the cleavage furrow during cytokinesis of the fission yeast, *Schizosaccharomyces pombe*. Pkd2p, whose human homologues are associated with autosomal polycystic kidney disease, is an essential protein whose localization depends on the contractile ring and the secretory pathway. We identified and characterized a novel *pkd2* mutant *pkd2-81KD*. The *pkd2* mutant cells show signs of osmotic stress, including temporary shrinking, paused turnover of the cytoskeletal structures, and hyperactivated mitogen-activated protein kinase signaling. During cytokinesis, although the contractile ring constricts more rapidly in the *pkd2* mutant than the wild-type cells (50% higher), the cell separation in the mutant is slower and often incomplete. These cytokinesis defects are also consistent with misregulated turgor pressure. Finally, the *pkd2* mutant exhibits strong genetic interactions with two mutants of the septation initiation network pathway, a signaling cascade essential for cytokinesis. We propose that Pkd2p modulates osmotic homeostasis and is potentially a novel regulator of cytokinesis.**

Monitoring Editor
Fred Chang
University of California, San Francisco

Received: May 7, 2018
Revised: Apr 29, 2019
Accepted: May 16, 2019

INTRODUCTION

Force plays a critical role in separating daughter cells during cytokinesis, the last stage of cell division (for review, see Pollard, 2010; Srivastava *et al.*, 2016). Since the initial discovery (Rappaport, 1967), studies by many groups have established that the actomyosin contractile ring is essential to generate the force required for cytokinesis (Sanger and Sanger, 1980; De Lozanne and Spudich, 1987; Straight *et al.*, 2003). What remains largely unknown is whether and how dividing cells respond to this force, a potential mechanical stimulus. Some have proposed that the activity of myosin II, a motor protein in the ring, may be force sensitive but the mechanism is far from clear (Effler *et al.*, 2006; Pinheiro *et al.*, 2017). On the other hand, few studies have examined whether any other mechanisms could contribute to force sensing during cytokinesis.

Mechanosensitive (MS) channels can open and close in response to mechanical force (for review, see Kung, 2005; Ranade *et al.*, 2015). The first such channel was identified in bacteria (Martinac *et al.*, 1987). Since then, many more MS channels have been found in not only prokaryotes but also eukaryotes including humans. Among them, the best studied examples are *Escherichia coli* MscS and MscL, which modulate intracellular osmolarity in response to hypoosmotic shocks (Sukharev *et al.*, 1994, 1996). Comparably, our understanding of eukaryotic MS channels such as PKD2, Piezo, and NompC is relatively limited, even though they are essential in sensing various forms of mechanical stimuli including flow, touch, and osmolarity (Mochizuki *et al.*, 1996; Walker *et al.*, 2000; Coste *et al.*, 2010). We have not completely understood how MS channels sense force, but two widely accepted models have been proposed (Kung, 2005; Arnadottir and Chalfie, 2010; Ranade *et al.*, 2015). The "Membrane tension" model hypothesizes that force directly

This article was published online ahead of print in MBoC in Press (http://www.molbiolcell.org/cgi/doi/10.1091/mbc.E18-04-0270) on May 22, 2019.

Author contributions: Q.C. designed the study. Z.M., D.S., A.P., B.M., and Q.C. carried out the experiments. Q.C. wrote the manuscript with input from Z.M., D.S., and A.P.

*Address correspondence to: Qian Chen (qian.chen3@utoledo.edu).

Abbreviations used: ADPKD, autosomal polycystic kidney disease; BFA, brefeldin A; LatA, latrunculin A; MAPK, mitogen-activated protein kinase; MBC, methyl benzimidazol-2-carbamate; SIN, septation initiation network; TRP, transient receptor potential.

stretches the membrane where MS channels are located to open their ion pores. The "Tethered" model proposes that force is applied to the extracellular matrix and/or the intracellular cytoskeleton to activate the MS channels indirectly. The functions of MS channels in nonsensory cells also remain largely unexplored.

We examined the potential roles of MS channels during cytokinesis using the fission yeast *Schizosaccharomyces pombe*. Classical genetics studies have identified a large number of important cytokinesis genes in this model organism (Balasubramanian *et al.*, 1998; Pollard and Wu, 2010; Johnson *et al.*, 2012). The molecular mechanism of fission yeast cytokinesis has been well studied and found to be largely conserved in higher eukaryotes (Pollard and Wu, 2010). Like animal cells, fission yeast assemble an actomyosin contractile ring at the cell division plane at the beginning of cytokinesis (Wu *et al.*, 2003). This process requires many essential proteins including Myo2p, Cdc12p, and Cofilin (Chang *et al.*, 1997; Balasubramanian *et al.*, 1998; Chen and Pollard, 2011) as well as continuous polymerization of the actin filaments (Courtemanche *et al.*, 2016). The ring assembly is followed by the contractile ring closure driven by the activities of both type II and type V myosins (Mishra *et al.*, 2013; Laplante *et al.*, 2015). The final step of cytokinesis is cell separation (for review, see Sipiczki, 2007; Garcia Cortes *et al.*, 2016), which includes such key steps as the septum biosynthesis (Liu *et al.*, 1999; Cortes *et al.*, 2002, 2012; Munoz *et al.*, 2013) and the cell wall degradation (Martin-Cuadrado *et al.*, 2003; Dekker *et al.*, 2004).

Mechanical forces, including that from the contractile ring, the septum, and the turgor, all play important roles during fission yeast cytokinesis. The tension originated from the contractile ring is required for the initiation of cell separation (Balasubramanian *et al.*, 1998; Mishra *et al.*, 2013; Stachowiak *et al.*, 2014). Just as importantly, the ring provides the mechanical cue that guides the septum biosynthesis (Thiyagarajan *et al.*, 2015; Zhou *et al.*, 2015). However, a recent work has shown that the ring is not required continuously during cytokinesis (Proctor *et al.*, 2012). The compression applied by the expanding septum helps both drive the cleavage furrow ingression and anchor the furrow at the cell division plane (Arasada and Pollard, 2014; Thiyagarajan *et al.*, 2015). This was vividly demonstrated by the observation that a defect in the septum biosynthesis often results in failed cell separation as well as postseparation cell lysis (Cortes *et al.*, 2012; Munoz *et al.*, 2013). Finally, the turgor pressure, essential to morphogenesis of yeast cells, plays a key but often underappreciated role in separating daughter cells (Proctor *et al.*, 2012; Abenza *et al.*, 2015; Atilgan *et al.*, 2015). Despite the importance of these forces, we have much to learn about how these mechanical stimuli are sensed and modulated during fission yeast cytokinesis, including the potential role of MS channels.

Here we examined the role of a putative transient receptor potential (TRP) channel Pkd2p during fission yeast cytokinesis. Many eukaryotic MS channels including NompC and human PKD2 belong to the TRP channel family (for review see Christensen and Corey, 2007). Consisting of seven subfamilies, this family of nonselective cation channels has been found in most eukaryotes (Wu *et al.*, 2010), including yeasts (Palmer *et al.*, 2001, 2005; Ma *et al.*, 2011). We discovered that a fission yeast TRP channel Pkd2p localizes to the cleavage furrow during cytokinesis. The *pkd2-81KD* mutation led to strong cytokinesis defects. Our genetic studies also identified the potential interaction between *pkd2* and the septation initiation network (SIN) pathway, a Hippo-like signaling cascade that regulates fission yeast cytokinesis (McCollum and Gould, 2001; Hergovich and Hemmings, 2012).

RESULTS

A putative TRP channel Pkd2p localizes to the cleavage furrow

To identify MS channels that may play a role during cytokinesis, we first determined whether any of the fission yeast TRP channels localize to the cell division plane (Palmer *et al.*, 2005; Aydar and Palmer, 2009; Ma *et al.*, 2011). The fission yeast genome encodes for the genes of three putative TRP channels, Pkd2p, Trp663p, and Trp1322p (Pombase). We tagged each of the endogenous proteins with GFP at its C-terminus (unless specified, mEGFP was used throughout this study). Only Pkd2p-GFP localized to the cell division plane prominently during cytokinesis (Figure 1A, Supplemental Figure S1A, and Supplemental Movie S1). The *pkd2::pkd2-GFP* cells exhibited similar morphology and viability to wild-type cells (unpublished data), indicating that Pkd2p-GFP is a functional replacement of the endogenous protein. We concluded that Pkd2p is a putative TRP channel localized at the cleavage furrow and it may have a role in cytokinesis.

We determined Pkd2p localization throughout cell cycle using live fluorescence microscopy. During cell division, Pkd2p-GFP first appeared at the cell division plane during telophase, ~30 min after separation of the spindle pole bodies (SPBs; Figure 1, B and C). Its molecular number gradually increased, eventually peaking at ~1200, when the ring closure was completed (Supplemental Figure S1C). Pkd2p-GFP localized to the intracellular vesicles and organelles. It was also found at the plasma membrane of cell tips (Figure 1D and Supplemental Movie S1) but it did not show a preference for either one of the tips (Figure 1D). We concluded that Pkd2p localization at the cell division plane is dependent upon cell-cycle progression.

We next examined how Pkd2p is recruited to the cleavage furrow during cytokinesis. First, we determined whether the actin or microtubule cytoskeletal structures are directly required for Pkd2p localization during cytokinesis. The actin cytoskeletal structures were disassembled within 5 min in the cells treated with 50 μM latrunculin A (Coue *et al.*, 1987; Chen and Pollard, 2013). However, Pkd2p-GFP remained at the cell division plane in these cells (Supplemental Figure S1D). Similarly, after the microtubules had been depolymerized in the cells treated by methyl benzimidazol-2-carbamate (MBC; Sawin and Snaith, 2004), Pkd2p localization at the division plane was unchanged (Supplemental Figure S1E). These observations demonstrated that neither actin filaments nor microtubules are required to maintain Pkd2p localization at the cleavage furrow. Next, we determined whether the contractile ring was required for Pkd2p localization. We dissembled the contractile ring by treating the cells with 10 μM latrunculin A for an extended period of time. In these cells, Pkd2p-GFP dispersed from the cleavage furrow to discrete puncta on the plasma membrane (Figure 1E). Consistent with this finding, Pkd2p also failed to localize to the cleavage furrow in *cdc12-112*, a mutant of the formin required for the ring assembly (Chang *et al.*, 1997), at the restrictive temperature (Figure 1F). Finally, we determined whether the secretory pathway is required for Pkd2p localization. Brefeldin A (BFA) was used to inhibit the secretory pathway (Misumi *et al.*, 1986). In these BFA-treated cells, Pkd2p-GFP localization to the cell division plane was inhibited (Supplemental Figure S1F). Together, our data suggested that Pkd2p localization at the cleavage furrow during cytokinesis requires both the contractile ring and the secretory pathway.

Pkd2 is an essential gene required for both cell growth and cell division

Pkd2p is the only fission yeast homologue of polycystins (Palmer *et al.*, 2005), an evolutionally conserved subfamily (TRPP) of TRP

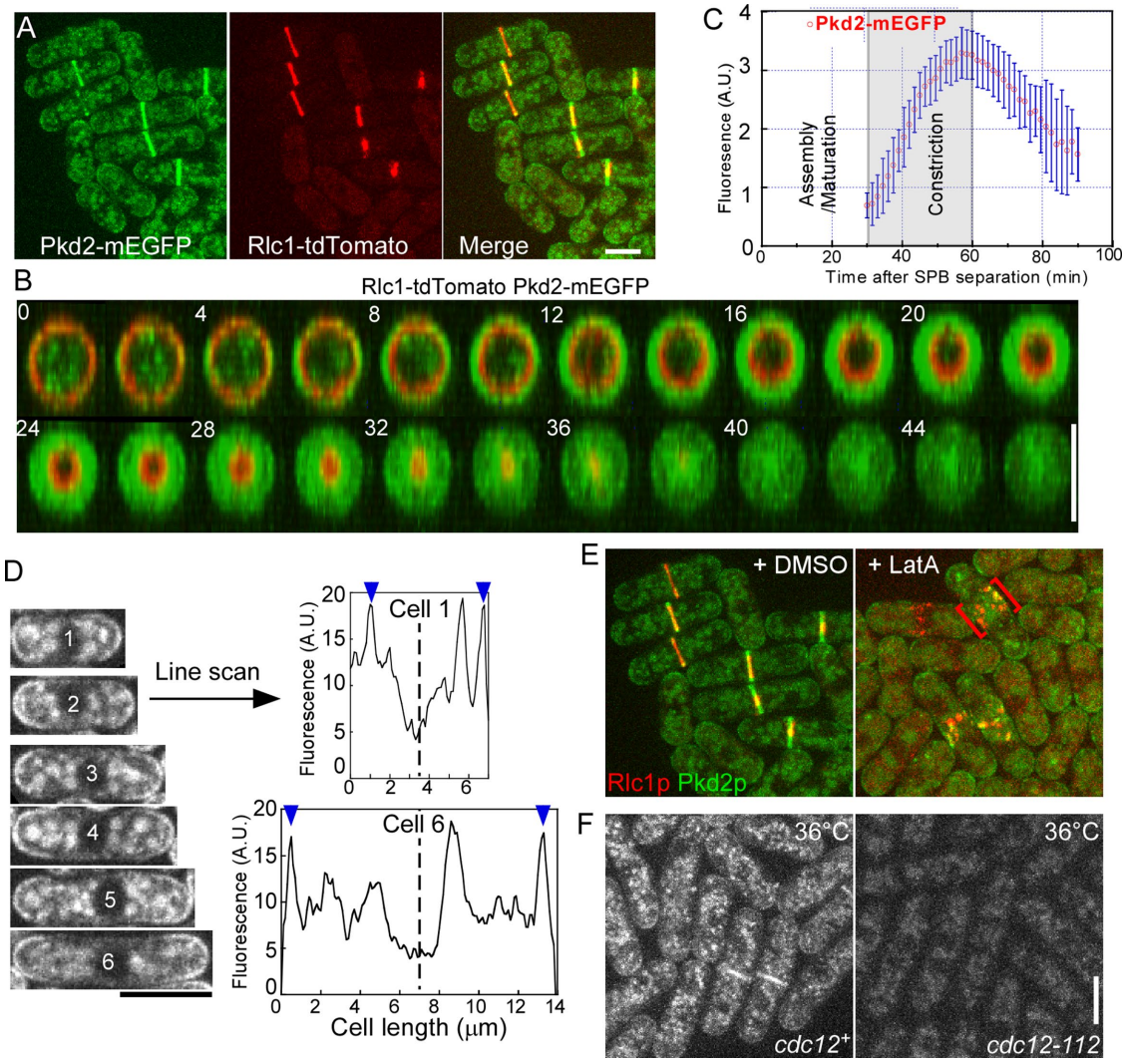

FIGURE 1: Localization of a TRP channel Pkd2p at the cell division plane. (A–C) Pkd2p localization during cytokinesis. (A, B) Fluorescence micrograph of cells expressing Pkd2p-GFP (green) and Rlc1p-tdTomoato (red), a marker for the contractile ring. Unless specified, maximum intensity projections are shown in all figures. (A) Fluorescence micrographs showing Pkd2p and Rlc1p colocalized to the contractile rings. Right, merged image. (B) Time-lapse micrographs of the division plane of a cell (head-on view and merged color). Numbers represent time in minutes. (C) Plot showing the time course of Pkd2p-GFP fluorescence at the cell division plane after the separation of SPBs (time zero). Pkd2p-GFP appeared at the division plane at the start of ring constriction (shaded area) and the fluorescence intensities peaked when the ring closure was completed. (D) Pkd2p localization during interphase. Left, fluorescence micrographs of six cells expressing Pkd2p-GFP (numbered from 1 to 6 based on their length). Average intensity projections of three center Z-slices are shown. Right, line scans based on the micrographs of cell 1 (top) and 6 (bottom). Pkd2p localized equally to the two cell tips (blue arrowheads). Dashed lines: median plane of the cells. (E, F) Regulation of Pkd2p localization. (E) Fluorescence micrographs of cells expressing Pkd2p-GFP (green) and Rlc1p-tdTomato (red), treated for 1 h with either control (dimethyl sulfoxide [DMSO], left) or 10 μM latrunculin A (LatA, right). Disassembly of the contractile ring displaced Pkd2p-GFP to the cortex clumps (red brackets). (F) Fluorescence micrographs of wild-type (*cdc12*$^{+}$) and *cdc12-112* cells expressing Pkd2p-GFP at 36°C. Pkd2p was displaced from the division plane at the restrictive temperature. Bars represent 5 μm. Error bars represent SD.

channels (Wu *et al.*, 2010). There are two human homologues of Pkd2p: PKD1 and the MS channel PKD2 (Hanaoka *et al.*, 2000; Nauli *et al.*, 2003). Mutations of either one of the human genes lead to a hereditary renal disorder, autosomal polycystic kidney disease (ADPKD). As a putative TRP channel, fission yeast Pkd2p possesses an N-terminal signal peptide, an extracellular lipid binding (ML-like) domain, a central transmembrane domain (TRP domain), and a C-terminal cytoplasmic coiled-coil domain (Figure 2, A and B). Pkd2p had been proposed to be a part of the cell wall integrity pathway (Palmer *et al.*, 2005; Aydar and Palmer, 2009) but its role in cytokinesis had not been characterized.

To determine the function of Pkd2p, we first attempted to construct a deletion mutant. However, *pkd2*Δ was not viable (Figure 2C), which agreed with the previous finding (Palmer *et al.*, 2005). In fact, microscopic examination of *pkd2*Δ spores found that the majority of them (24/26) failed to divide and died before initiating polarized outgrowth (Figure 2D), although few of the mutant spores (2/26) did divide one to two rounds before death (Figure 2D). We

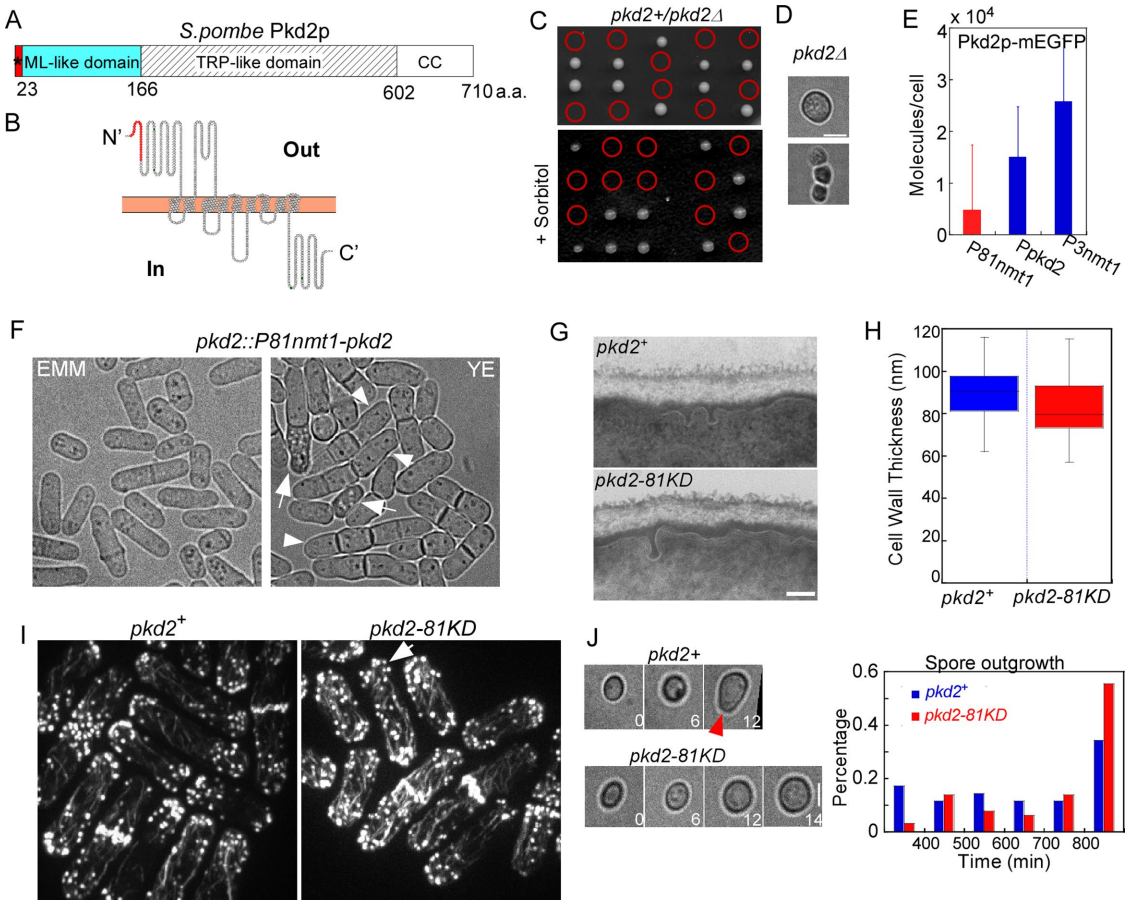

FIGURE 2: An essential gene *pkd2* is required for cell growth and cell division. (A, B) Putative TRP channel Pkd2p. (A) Domain structure of Pkd2p. *: the signal peptide. ML-like: MD-2–related lipid recognition domain. TRP-like: the transmembrane domain. CC: coiled-coil domain. (B) Predicted topology of Pkd2p on the plasma membrane (orange). Red: the signal peptide. Pkd2p is projected to contain extensive extracellular and cytoplasmic domains. (C, D) *pkd2* is an essential gene. (C) Tetrad dissections of sporulated *pkd2*$^+$/*pkd2*Δ cells, germinated on either YE5s (top) or YE5s plus 1.2 M sorbitol plates (bottom). Red circles: expected *pkd2*Δ spores. The *pkd2* deletion mutant is not viable. (D) Representative micrographs of *pkd2*Δ spores germinated on YE5s for more than 1 wk. Most mutant spores died during the outgrowth (top) although a small number died after one to two rounds of cell division (bottom). Compared to wild-type spores that initiated polarized outgrowth (J), *pkd2*Δ spores grew isotropically. (E–J) Characterization of a hypomorphic *pkd2* mutant. (E) Bar graph comparing the average number of Pkd2p-GFP molecules per cell among *pkd2::P81nmt1-pkd2-GFP* (P81nmt1), *pkd2-GFP* (Ppkd2), and *pkd2::P3nmt1-pkd2-GFP* (P3nmt1) in YE5s ($n > 60$). Replacing the endogenous *pkd2* promoter with P81nmt1 reduced the number of Pkd2p molecules by 70%, while P3nmt1 promoter increased the molecular number onefold. (F) Micrographs of *pkd2-81KD* cells in either YE5s (suppressing) or EMM5s (inducing) media. Under suppressing condition, many mutant cells were multiseptated (arrowheads) and some appeared to be lysed (arrows). Both morphological defects were rescued under inducing condition. (G) Transmission electron micrographs of the cell wall of a wild-type (top) and a *pkd2-81KD* (bottom) cell. (H) Box plot showing the average thickness of wild-type and *pkd2-81KD* cell walls ($n > 8$ cells). There was no significant difference between them ($P > 0.05$). (I) Fluorescence micrographs of bodipy-phallacidin stained wild-type (left) and *pkd2-81KD* (right) cells. Distribution of the actin patches (arrow) was less polarized in the mutant cells, even though their actin cytoskeletal structures appeared to be similar to those of the wild-type cells. (J) Left, representative time-lapse micrographs of a wild-type (top) and a *pkd2-81KD* (bottom) spore after germination (time zero). Numbers represent time in hours. Right, histogram showing the elapsed times before the initiation of polarized outgrowth (arrowhead). The outgrowth of *pkd2-81KD* mutant (red) was delayed, compared with the wild-type spores (blue; $n > 30$). All error bars represent SD.

attempted to rescue the deletion mutant with an osmotic stabilizer because of its proposed role in the cell wall integrity pathway. However, *pkd2*Δ did not survive in the presence of 1.2 M sorbitol (Figure 2C). We concluded that *pkd2* is an essential gene, required for cell growth and cell division.

Next, we attempted to construct a viable *pkd2* mutant. We replaced the endogenous *pkd2* promoter with a series of inducible promoters (Maundrell, 1990; Basi *et al.*, 1993). Among the three resulting *pkd2* mutants, the one with the strongest growth defect is *pkd2::P81nmt1-pkd2* (referred to as *pkd2-81KD*; Supplemental Figure S2A), in which a weak inducible *81nmt1* promoter replaced the endogenous promoter. The *pkd2-81KD* mutant was also hypersensitive to high concentration of salts including $CaCl_2$ (Supplemental Figure S2B). To quantify the depletion or overexpression of

Pkd2p in the mutants, Pkd2p was tagged with GFP in both *pkd2-81KD* and *pkd2::P3nmt1-pkd2* to measure average numbers of Pkd2p molecules per cell (Supplemental Figure S2C and Supplemental Movie S2). The number of Pkd2p molecules decreased by ~70% in the *pkd2-81KD* cells but doubled in *pkd2::P3nmt1-pkd2*, when the *nmt1* promoters were suppressed (Figure 2E). The depletion of Pkd2p led to strong morphological defects of *pkd2-81KD* cells, which could be reversed by removing thiamine to restore the expression of *pkd2* (Figure 2F). In contrast, neither *trp663*Δ nor *trp1322*Δ cells exhibited an apparent morphological defect (Supplemental Figure S1B). We concluded that *pkd2-81KD* is a novel hypomorphic *pkd2* mutant that can be used in further studies of this gene.

We examined the *pkd2-81KD* mutant for its other defects. The mutant cells were significantly wider than the wild-type cells (Supplemental Figure S2D). The cell wall of this *pkd2* mutant, examined with transmission electron microscopy, was similar in appearance and thickness to that of the wild type (Figure 2, G and H). Compared to the wild-type cells, the actin cytoskeletal structures of the mutant appeared to be similar, but distribution of the interphase actin patches was less polarized in the mutant cells, suggesting a potential cell polarity defect (Figure 2I). The requirement of Pkd2p was not limited to vegetative cells. The *pkd2* mutant spores initiated their outgrowth more slowly than the wild-type ones did (Figure 2J), reminiscent of the defect observed in *pkd2*Δ spores noted above. This germination defect of the *pkd2-81KD* spores was also apparent in their usual slow growth following tetrad dissections (unpublished data). We concluded that Pkd2p likely plays an essential role in cell morphogenesis.

Temporary deflation of the *pkd2* mutant cells

When examining *pkd2-81KD* cells with bright-field microscopy, we noticed that some of them appeared to be lysed. Because cell lysis is often associated with a defect in the cell wall biosynthesis, we characterized this phenotype in further details (Cortes *et al.*, 2012; Munoz *et al.*, 2013; Davidson *et al.*, 2016; Sethi *et al.*, 2016). To our surprise, these mutant cells did not lyse completely but they merely shrank temporarily, which we termed as "Deflation," before quickly recovered. In all, 16% of the mutant cells underwent deflation and reinflation (Figure 3A and Supplemental Movie S3). In contrast, no wild-type cell shrank under the same condition. The temporary deflation of the *pkd2* mutant cells lasted ~20 min (20 ± 8 min, average ± SD, $n = 12$) during which the cell size was reduced by ~20% (Figure 3D). Interestingly, the majority of deflated cells were not undergoing either cell division or septation (80%, $n = 15$), suggesting that neither triggered the deflation. To our knowledge, this unique phenotype has not been described before for any other mutant. The quick loss of cell volume and the following recovery to some extent resembled the response of wild-type cells to hypertonic stress.

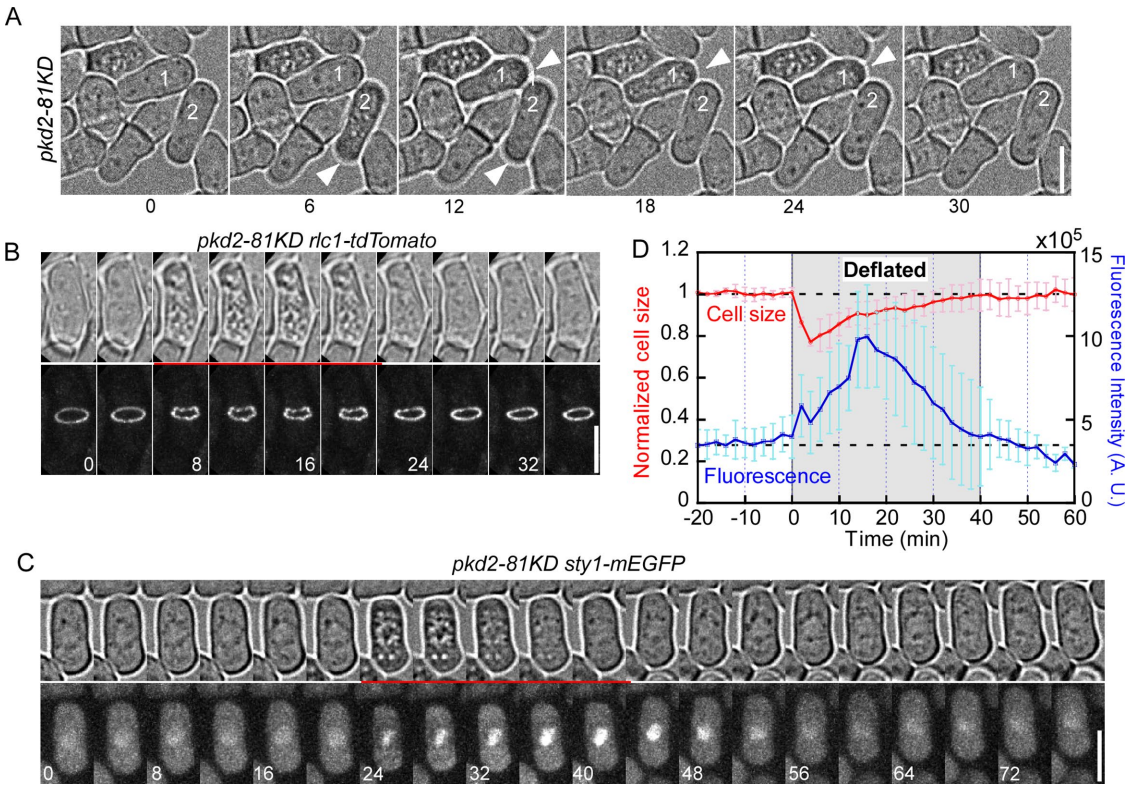

FIGURE 3: Deflation of the *pkd2* mutant cells. (A) Time-lapse micrographs of *pkd2-81KD* cells. Both cells 1 and 2 shrank temporarily (arrowheads). Numbers represent time in minutes. (B) Time-lapse micrographs of a *pkd2-81KD* cell expressing Rlc1p-tdTomato. The ring transformed into a "wavy band" (bottom) during the period of temporary deflation (top, red underline). (C) Time-lapse micrographs of a *pkd2-81KD* cell expressing Sty1p-GFP. Temporary shrinking (top, red underlined) of the cell was concomitant with increased Sty1p-GFP localization in the nucleus (bottom). Number represents time in minutes. (D) Plot showing the time courses of average sizes (red line, normalized) and nuclear Sty1p-GFP fluorescence (blue line) of *pkd2-81KD* cells ($n = 7$). The shrinking reduced the average cell size by ~20%. Concurrently, Sty1p-GFP fluorescence in the nucleus increased by about threefold. Error bars represent SD.

We determined whether deflation of the *pkd2* mutant cells was a result of osmotic stress by first examining turnovers of their cytoskeletal structures which would stop temporarily in response to osmotic stresses (Robertson and Hagan, 2008). We first examined the contractile ring and the actin patches, two actin cytoskeletal structures. Upon deflation of the mutant cells, their contractile ring stopped constricting abruptly and converted temporarily from a circular ring into a "wavy band" (Figure 3B and Supplemental Movie S4). The deflation triggered a stop in turnover of the endocytic actin patches as well (Supplemental Figure S3A). Not surprisingly, turnover of the microtubules stopped temporarily in the deflated cells too (Supplemental Figure S3B and Supplemental Movies S5 and S6). We concluded that turnover of the cytoskeletal structures was stopped temporarily in the deflated *pkd2* mutant cells as in osmotic stressed cells.

We next determined whether deflation of the *pkd2* mutant cells also activated the Sty1p-mediated mitogen-activated protein kinase (MAPK) pathway, another hallmark of the cells under osmotic stresses. Activation of this MAPK pathway shuttles Sty1p into the nucleus where the kinase mediates the stress-activated gene expressions (Millar *et al.*, 1995; Shiozaki and Russell, 1995; Degols *et al.*, 1996). We found significantly more Sty1p-GFP molecules in the nuclei of *pkd2-81KD* cells than the wild-type cells (Supplemental Figure S3, C and D). When the *pkd2* mutant cells shrank, nuclear localization of Sty1p-GFP increased concomitantly by up to three folds, compared with predeflation (Figure 3, C and D, and Supplemental Movie S7). We concluded that the Sty1p-mediated MAPK pathway was hyperactivated during deflation of the *pkd2* mutant cells as was found in osmotically stressed cells. In addition, we also found that the deflation of *pkd2* mutant cells could be rescued by the osmotic stabilizer sorbitol ($n > 500$ cells; Supplemental Figure S3E). In summary, we concluded that Pkd2p most likely regulates osmotic homeostasis during cell growth.

Pkd2p regulates the ring closure during cytokinesis

To examine the role of Pkd2p during cytokinesis, we first measured the contractile ring assembly in *pkd2-81KD* cells. Overall, the ring assembled normally in the mutant cells (Supplemental Movies S8 and S9). The *pkd2* mutation did not disrupt the placement of rings at the cell division plane (Figure 4A). The rings were positioned properly in the *pkd2* mutant cells as well, unlike the oblique angled rings found in those mutants with a defect in the septum biosynthesis (Munoz *et al.*, 2013). We did notice that the mutant cells were significantly shorter than the wild-type cells during cytokinesis (Figure 4B). The *pkd2* mutant cells also experienced a slight but significant delay in ring assembly and maturation, compared with the wild-type cells (Figure 4C; 29 ± 4 vs. 25 ± 4 min, average ± SD, $P < 0.001$). We concluded that Pkd2p is not essential for either the assembly or maturation of the contractile ring.

Next, we determined whether Pkd2p regulates ring closure, a more likely role considering its localization during cytokinesis. Surprisingly, ring closure on average took less time in the mutant than in the wild-type cells (Figure 4D), in spite of our earlier observation that the mutant cells were wider than the wild-type ones (Supplemental Figure S2D). As expected, the rings in the mutant cells contracted more than 50% faster than they did in the wild-type cells (Figure 4, E and F, and Supplemental Figure S4A; 0.47 ± 0.07 vs. 0.30 ± 0.04 μm/min, $P < 0.0001$). Our measurement of ring closure in the wild-type cells, closely matched the previously published values (Chen and Pollard, 2011; Proctor *et al.*, 2012; Laplante *et al.*, 2015). We did not observe any sliding of the rings during their contraction in the mutant ($n > 50$), which would have occurred if the ring had not been anchored properly (Cortes *et al.*, 2012; Arasada and Pollard, 2014). Therefore, it was unlikely that this rapid ring closure in the mutant was a result of failure to couple the ring to the plasma membrane or the cell wall. Unexpectedly, overexpression of Pkd2p did not slow the ring closure as one would have predicted (Supplemental Figure S4, B and C), indicating that Pkd2p is necessary, but not sufficient in modulating the rate of ring closure. We concluded that Pkd2p modulates ring closure during cytokinesis but is dispensable for ring assembly, maturation, or anchoring.

Pkd2p is required for separation of daughter cells

We next examined the role of Pkd2p in cell separation, the final phase of fission yeast cytokinesis. Two lines of evidence indicated that Pkd2p may play an important role in cell separation. First, the fraction of *pkd2-81KD* cells with septa was about three times higher than the wild-type cells (Figure 5, A and B). In addition, close to 9% of the mutant cells were multiseptated (Figure 5B). We also noticed that the septum in these multiseptated mutant cells frequently swung from one side to another at a rate of 0.05 ± 0.03 μm/min ($n = 12$). Second, the septa in many mutant cells were curved, deposited ectopically at the cell tips or unusually thick (Figure 5A). We postulated that Pkd2p is likely essential for cell separation.

We examined separation of the *pkd2* mutant cells during cytokinesis with live microscopy. The wild-type cells reliably separated in ~30 min (28 ± 5 min, average ± SD, $n = 20$) after completion of the ring closure (Figure 5C). In contrast, the mutant cells took more than twice as long (Figure 5D; 75 ± 21 min, $n = 17$) with some of them taking as long as 120 min to separate (Figure 5C). Furthermore, some mutant cells failed to separate completely, explaining the many multiseptated *pkd2* mutant cells. Wild-type cells typically separate symmetrically by detaching both sides of the new ends from each other simultaneously (Figure 5C). In contrast, most mutant cells separated asymmetrically by usually detaching one side of the new ends first (Figure 5C, bottom row). We concluded that Pkd2p plays an essential role in separating the new ends during cell separation.

We next determined whether Pkd2p was required for either the septum biosynthesis or the cell wall degradation, two critical steps of cell separation. We first examined the localization of two glucan synthases Bgs1p and Bgs4p, both of which are required for the septum biosynthesis (Le Goff *et al.*, 1999; Liu *et al.*, 1999; Cortes *et al.*, 2007). Both GFP-Bgs1p and GFP-Bgs4p still localized to the cell division plane in the *pkd2-81KD* cells, as they did in the wild-type cells (Figure 6, A and B). Furthermore, the time course of recruitment and dispersal of either Bgs1p or Bgs4p at the division plane in the mutant remained largely unchanged as well (Figure 6, C and D). The septum did close more rapidly in the mutant compared with the wild-type cells, consistent with the quicker ring closure in the mutant (Supplemental Figure S4, D and E). As a result, the number of Bgs1p molecules at the cell division plane of the mutant decreased slightly compared with the wild-type cells (Figure 6C). In contrast, the number of GFP-Bgs4p molecules at the division plane rose slightly (Figure 6D). We concluded that Pkd2p is dispensable for the localization of these two glucan synthases during cell separation. Next, we determined whether Pkd2p is required for the localization of Eng1p, a glucanase that degrades the septum at the end of cell separation (Martin-Cuadrado *et al.*, 2003; Sipiczki, 2007). The *pkd2* mutation did not alter the localization of Eng1p-GFP at the cell division plane (Supplemental Figure S4, F and G). The number of Englp-GFP molecules at the division plane remained unchanged, compared with that in the wild-type cells. We concluded that Pkd2p is not required for the localization of Eng1p either and the most

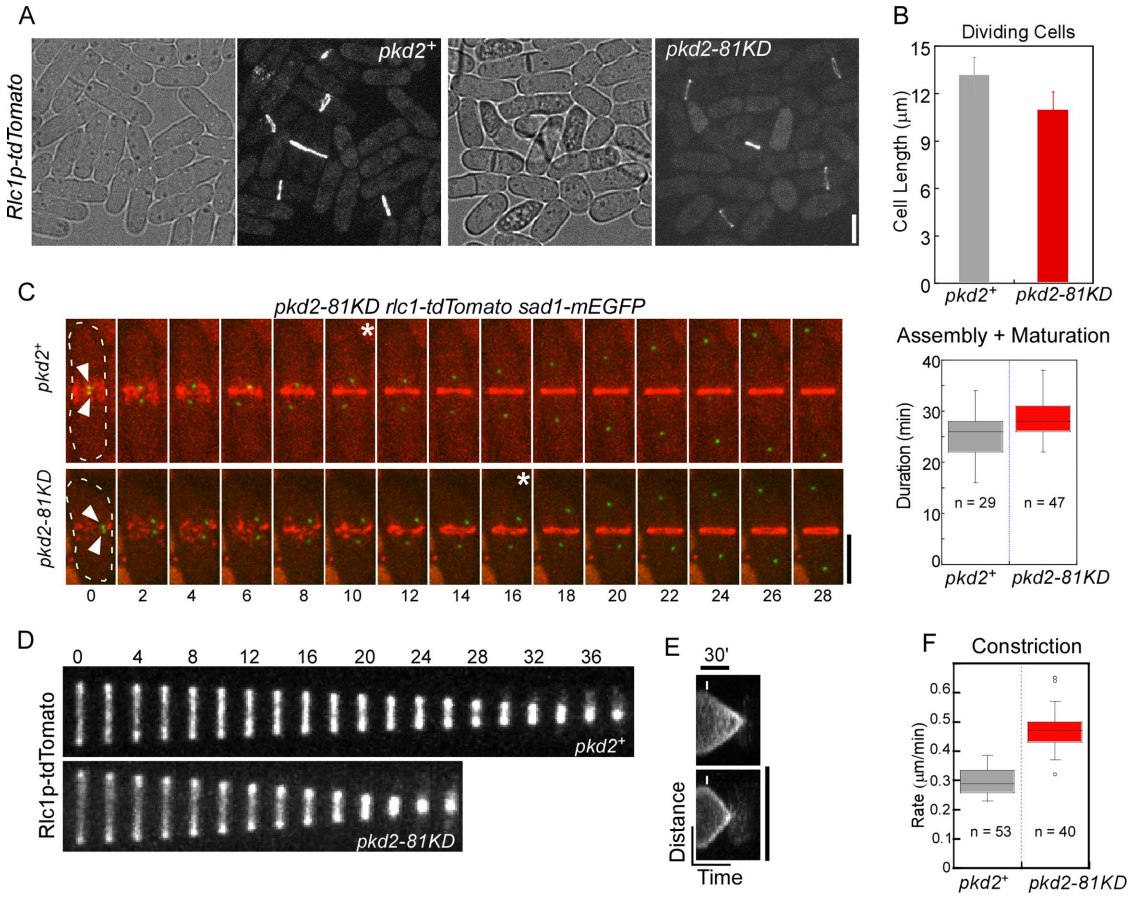

FIGURE 4: Increased ring closure rate in *pkd2-81KD* cells. (A) Micrographs of wild-type (*pkd2*$^+$, left) and *pkd2-81KD* (right) cells expressing Rlc1p-tdTomato. Placement of the contractile rings in the mutant was similar to that in the wild-type cells. (B) Bar graph showing the average length of wild-type and *pkd2-81KD* cells during cytokinesis. The analysis included only cells with one complete contractile ring. The *pkd2* mutant cells were significantly shorter than the wild-type cells ($n > 50$, $P < 0.001$). (C) Ring assembly in *pkd2-81KD* cells. Left, time-lapse fluorescence micrographs of a wild-type (top, *pkd2*$^+$) and a *pkd2-81KD* (bottom) cell. Both cells expressed Rlc1p-tdTomato (red) and Sad1p-GFP (green), a marker for SPBs (arrowheads). Ring assembly was slower in the mutant (~6 min) than the wild-type cells. Asterisks indicate the appearance of a complete ring. Numbers represent time in minutes. Right, box plot showing the duration of ring assembly plus maturation in wild-type (gray) and *pkd2-81KD* cells (red). Ring assembly and maturation was slower in the mutant compared with the wild-type cells ($P < 0.0001$). (D–F) Ring closure in *pkd2-81KD* cells. Time-lapse fluorescence micrographs of the cell division plane in a wild-type (top) and a *pkd2-81KD* (bottom) cell. Frame interval is 2 min. The rings constricted more rapidly in the mutant than in the wild-type cells. (E) Fluorescence kymographs of ring closure in a wild-type (top) and a *pkd2* mutant (bottom) cell. Lines: Start of ring closure. (F) Box plot showing the average ring closure rates in wild-type (gray) and *pkd2-81KD* (red) cells. The rate increased by ~50% in the mutant. Bars represent 5 μm. Error bars represent SD.

likely role of Pkd2p during cell separation is to regulate the turgor pressure in the separation of new ends.

Genetic interactions between *pkd-81KD* and the other cytokinesis mutants

Pkd2p localization at the cleavage furrow and its role in cell separation prompted us to examine whether it interacts with the other cytokinesis genes. We carried out a targeted screen to identify genetic interactions between *pkd2-81KD* and 11 other cytokinesis mutants (Figure 7A). Four of them interacted negatively with the *pkd2* mutant (Figure 7A), including the temperature-sensitive mutants of *myo2* (type II myosin), *cdc12* (formin), *rng2* (IQGAP1 homologue), and *cdc15* (a F-BAR protein), respectively. All four genes are required for the ring assembly (Fankhauser *et al.*, 1995; Chang *et al.*, 1997; Kitayama *et al.*, 1997; Eng *et al.*, 1998). On the other hand, *cps1-191*, the temperature-sensitive mutant of *bgs1*, exhibited no genetic interaction with *pkd2-81KD* mutant. We concluded that Pkd2p plays a synergistic role with Myo2p, Cdc12p, Rng2p, and Cdc15p during cytokinesis.

Two SIN mutants, *mob1-R4* and *sid2-250*, had the strongest genetic interactions with *pkd2-81KD*. They are the temperature-sensitive mutants of Sid2p kinase and its activator Mob1p, respectively (Balasubramanian *et al.*, 1998; Hou *et al.*, 2000). Growth of *mob1-R4* was rescued by the *pkd2* mutation at the restrictive temperature (Figure 7B). In comparison, the *pkd2* mutation only rescued the growth of *sid2-250* at semirestrictive temperature. The SIN temperature-sensitive mutants failed in septation and eventually lysed, at the restrictive temperature (Figure 7, C and D; Balasubramanian *et al.*, 1998; Salimova *et al.*, 2000; Krapp *et al.*, 2004). The *pkd2-81KD* mutation prevented the lysis of both SIN mutant cells (Figure 7E and Supplemental Figure S5C). Additionally, the relatively mild septation defect of *mob1-R4* cells was also rescued by

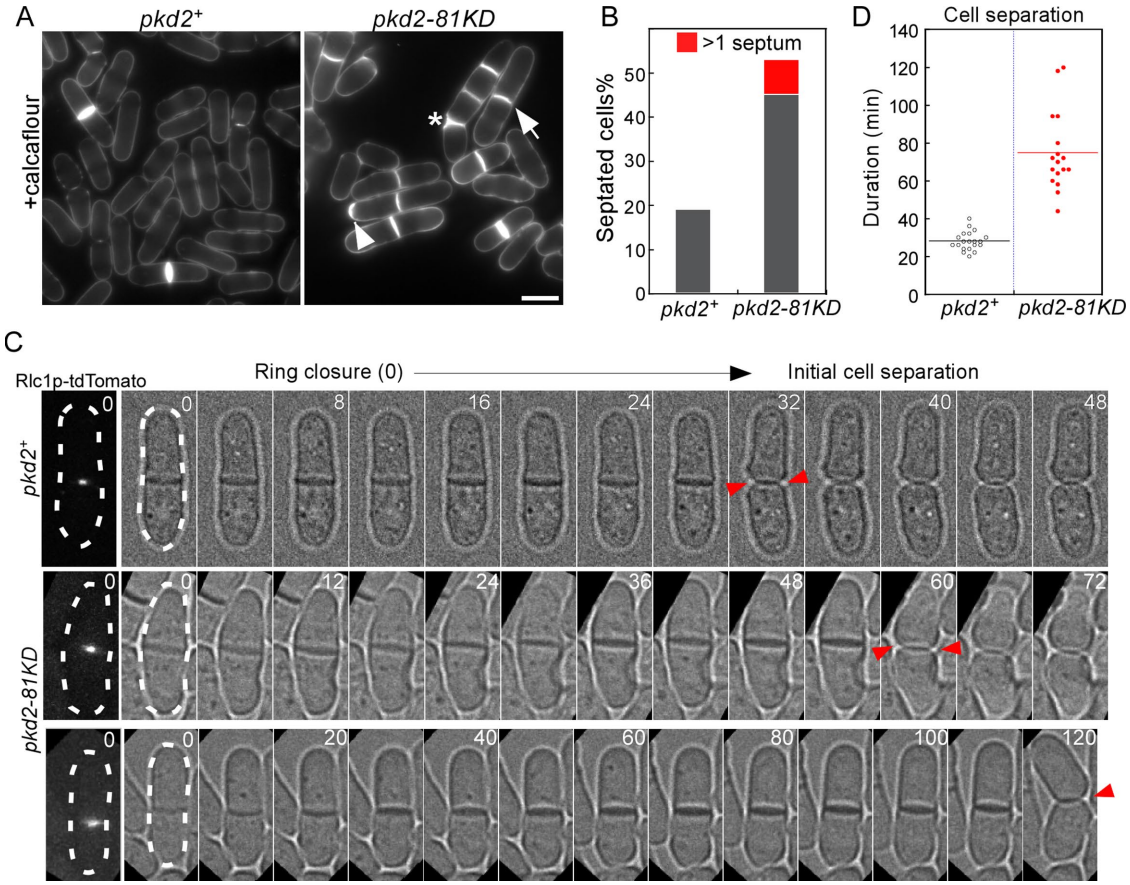

FIGURE 5: Separation defect of *pkd2-81KD* cells during cytokinesis. (A) Fluorescence micrographs of calcofluor-stained wild-type (*pkd2*$^+$, left) and *pkd2-81KD* (right) cells. Septum of the mutant cells were often curved (arrow), thicker than normal (asterisk), or deposited ectopically (arrowhead). (B) Bar graph showing the percentage of wild-type and *pkd2-81KD* cells with at least one septum ($n > 500$). The percentage of multiseptated cells is shown in red. The fraction of septated *pkd2-81KD* cells was almost three times higher than that of the wild-type cells. (C, D) Separation defect of the *pkd2* mutant cells. (C) Time-lapse micrographs of a wild-type (top) and two *pkd2-81KD* (middle and bottom) cells. All three cells expressed Rlc1p-tdTomato. Left, fluorescence micrographs of the cell when the ring closure was completed (time zero). Numbers represent time in minutes. Frame intervals are 4 (top), 6 (middle), and 10 (bottom) min, respectively. The wild-type cell took 32 min to separate (red arrowheads). In contrast, the two *pkd2-81KD* cells took 60 and 120 min, respectively. (D) Dot plot showing the durations of cell separation in wild-type and *pkd2-81KD* cells ($n > 15$). The horizontal lines represent averages. The mutant cells separated more slowly than the wild-type cells.

pkd2-81KD (Figure 7F and Supplemental Figure S5D). In comparison, the septation defect of *sid2-250* mutant was only partially rescued by the *pkd2* mutation at both semirestrictive and restrictive temperature (Figure 7F and Supplemental Figure S5D). Additionally, the septa of *sid2-250 pkd2-81KD* cells were much thinner than those of wild-type cells (Figure 7C). We concluded that Pkd2p and the SIN pathway play antagonistic roles in septation and maintaining cell integrity.

DISCUSSION

Forces, generated by the contractile ring, the septum, and the turgor, are essential for fission yeast cytokinesis. However, we know relatively little about how these forces can be sensed and modulated by cells. Here we showed that a putative force-gated channel Pkd2p has several important functions during cytokinesis, including modulating the ring closure and promoting cell separation. Defects of the *pkd2-81KD* mutant cells suggest that the most likely role of this TRP channel is to regulate osmotic homeostasis. Not surprisingly, Pkd2p is well placed at the cleavage furrow during cytokinesis to execute this function. The genetic interactions between *pkd2-81KD* and the other cytokinesis mutants also support that this transmembrane protein may be a novel component of the cytokinetic machinery.

Localization of Pkd2p channel at the cleavage furrow

To our knowledge, Pkd2p is the first putative ion channel that localizes to the cell division plane of fission yeast cells. Our discovery is compatible with the previous finding that Pkd2p was mostly found at the intracellular organelles and the plasma membrane (Palmer *et al.*, 2005; Aydar and Palmer, 2009). Pkd2p is one of the few TRP channels that have been found at the cleavage furrow so far. TRP3 channel of the zebrafish *Danio rerio*, which mediates the influx of calcium at the furrow, is the other notable example (Chan *et al.*, 2015). Many molecules in the contractile ring may interact with Pkd2p directly to recruit it to the cleavage furrow. This mechanism will be consistent with our observation that the contractile ring is required for Pkd2p localization. The septum may also interact with Pkd2p directly, considering that the initial appearance of Pkd2p at

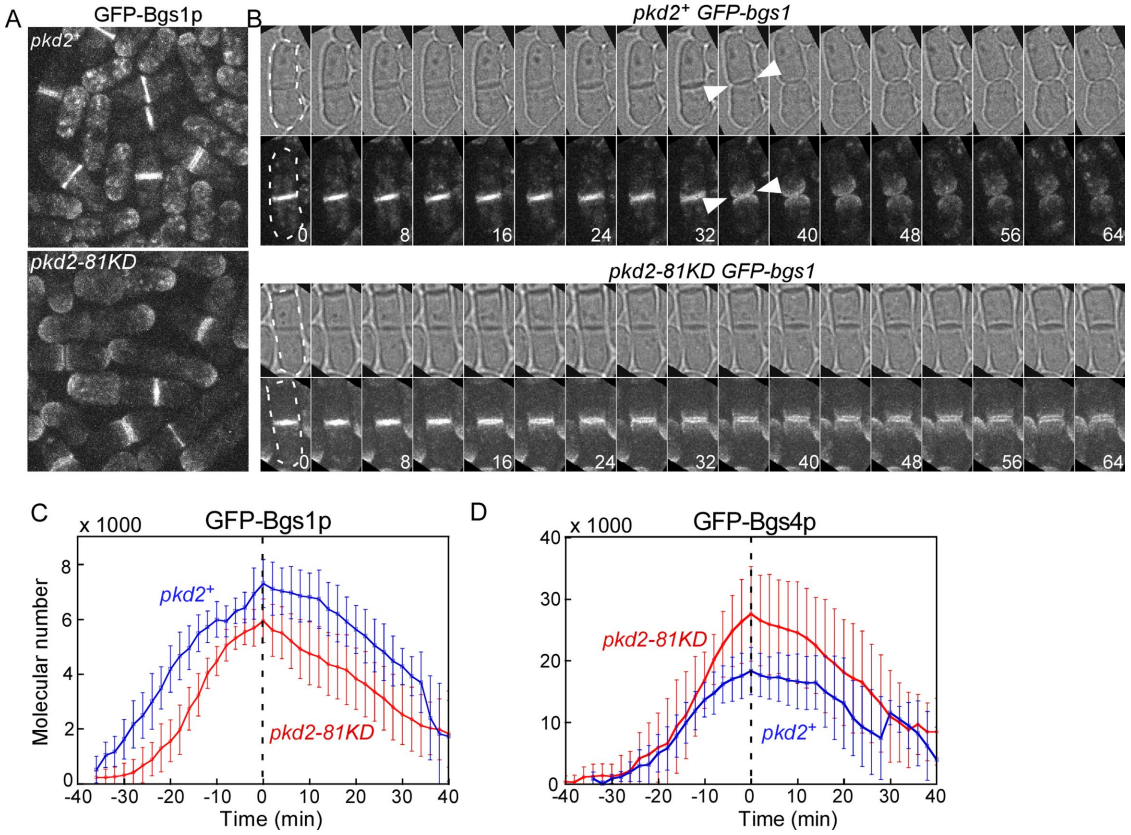

FIGURE 6: Localization of the glucan synthases Bgs1p and Bgs4p in *pkd2-18KD* cells. (A) Fluorescence micrographs of wild-type (*pkd2*$^+$, top) and *pkd2-81KD* (bottom) cells expressing GFP-Bgs1p. The *pkd2* mutation did not alter GFP-Bgs1p localization at the cell division plane. (B) Time-lapse micrographs of a wild-type (top) and a *pkd2-81KD* (bottom) cell expressing GFP-Bgs1p. The wild-type cells separated at 36 min (white arrowheads) after the ring closure (time zero), but the mutant cells failed to separate. Nevertheless, GFP-Bgs1p localization at the cell division plane appeared unchanged in the mutant. Frame interval is 4 min. Numbers represent time in minutes. (C, D) Line plots showing the time courses of GFP-Bgs1p (C) and GFP-Bgs4p (D) molecules localized at the division plane of either wild-type (blue line) or *pkd2-81KD* cells (red line). The number of GFP-Bgs1p molecules in the *pkd2* mutant was slightly reduced but the number of GFP-Bgs4p molecules was increased, compared with the wild-type cells ($n > 5$). Error bars represent SD.

the furrow coincides with the start of primary septum synthesis. Future studies will be needed to determine the molecular mechanism of Pkd2p recruitment to the cell division plane.

Based on our study of fission yeast Pkd2p, it will be interesting to determine the localization of other Pkd2p homologues during cytokinesis. Budding yeast homologues of Pkd2p localize to both the ER and plasma membrane (Protchenko *et al.*, 2006) but their localization during cytokinesis has not been examined. Among the two human Pkd2p homologues, PKD1 is primarily localized at the plasma membrane (Hughes *et al.*, 1995) and PKD2 is mostly found on the ER membrane (Gonzalez-Perrett *et al.*, 2001), although PKD2 does localize to the mitotic spindles through its interaction with formin mDia1 in cultured kidney epithelial cells (Rundle *et al.*, 2004). Additionally, most Pkd2p homologues, including those of humans, *Caenorhabditis elegans*, and *Drosophila melanogaster*, also localize to the cilia of nondividing cells (Barr and Sternberg, 1999; Barr *et al.*, 2001; Pazour *et al.*, 2002; Yoder *et al.*, 2002; Gao *et al.*, 2003; Nauli *et al.*, 2003; Watnick *et al.*, 2003). Future work would be necessary to determine the cytokinetic localization of Pkd2p in dividing animal cells.

Molecular functions of Pkd2p during cytokinesis

Our study suggests that Pkd2p most likely regulates osmotic homeostasis during cytokinesis as well as cell morphogenesis. This model is supported by at least three lines of evidence. First, the unique deflation defect of the *pkd2* mutant could be due to a defect in the regulation of turgor pressure. The temporary shrinking of *pkd2-81KD* cells activated the stress response pathway mediated by Sty1p. The shrinking also stopped turnovers of all cytoskeletal structures that we examined. All of these phenotypes are consistent with misregulated turgor pressure. In addition, the septa of multiseptated *pkd2-81KD* cells often swung from side to side, suggesting that turgor pressure fluctuates drastically in these mutant cells. Second, the morphology of *pkd2-81KD* cells also imply a defect in the osmotic regulation during cell morphogenesis. Compared to wild-type cells, the *pkd2* mutant cells are shorter but wider and the distribution of their actin patches is partially depolarized. Furthermore, both *pkd2*Δ and *pkd2-81KD* spores either failed or delayed their outgrowth during germination. These observations are consistent with a defect in the regulation of turgor pressure, which is essential to fission yeast cell growth (Atilgan *et al.*, 2015; Davi *et al.*, 2018). Third, the cytokinesis defects of *pkd2-81KD* cells are also consistent with misregulated turgor pressure. Both rapid ring and septum closure in the mutant cells can be a result of low turgor pressure, which could reduce resistance to the furrow ingression and increase the ring closure rate, compared with the wild-type cells. This hypothesis is

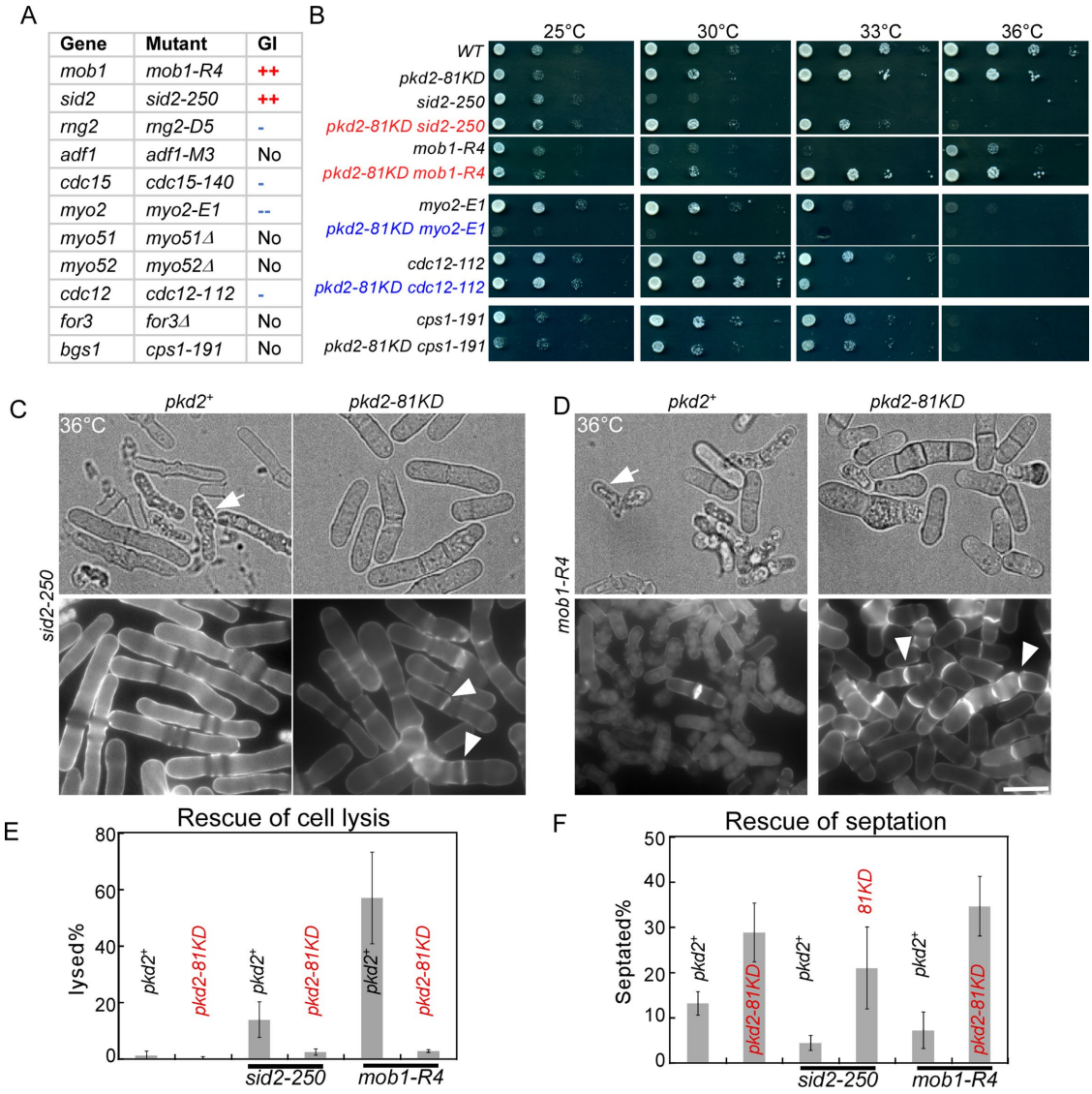

Gene	Mutant	GI
mob1	*mob1-R4*	++
sid2	*sid2-250*	++
rng2	*rng2-D5*	-
adf1	*adf1-M3*	No
cdc15	*cdc15-140*	-
myo2	*myo2-E1*	--
myo51	*myo51Δ*	No
myo52	*myo52Δ*	No
cdc12	*cdc12-112*	-
for3	*for3Δ*	No
bgs1	*cps1-191*	No

FIGURE 7: Genetic interactions between *pkd2-81KD* and the other cytokinesis mutants. (A) Table summarizing the genetic interactions (GI) between *pkd2-81KD* and 11 other cytokinesis mutants. Positive interactions are designated by either "++" (strong), whereas negative interactions are designated by either "--" (strong) or "-" (weak). "NO" indicates no genetic interactions. (B) Tenfold dilution series of yeast cells at the indicated temperatures. *pkd2-81KD* mutant had positive genetic interactions with *mob1-R4* and *sid2-250* but negative interactions with *myo2-E1* and *cdc12-112*. It had no genetic interactions with *cps1-191*. (C, D) Micrographs of *sid2-250*, *sid2-250 pkd2-81KD*, *mob1-R4*, and *mob1-R4 pkd2-81KD* cells grown at 36°C. Top, bright-field micrographs of the live cells. Bottom, fluorescence micrographs of the calcofluor-stained cells. Arrows: lysed cells. Arrowheads: the septum. The SIN mutants frequently lysed and few of them contained septum at the restrictive temperature, defects that were partially rescued by the *pkd2* mutation. (E, F) Bar graphs showing the percentage of either lysed (E) or septated (F) cells at 36°C. The *pkd2* mutation largely rescued both the lysis and septation defects of the SIN mutants. Error bars represent SD.

consistent with the important role of turgor in determining ring closure rate (Proctor *et al.*, 2012). On the other hand, slow or failed separation of the *pkd2* mutant cells may be attributed to misregulated turgor at the cell division plane (Sipiczki, 2007; Abenza *et al.*, 2015; Atilgan *et al.*, 2015). Although future studies will be necessary to directly measure the putative abnormities of turgor pressure in the *pkd2* mutation cells, our observations strongly support that Pkd2p plays an essential role in osmotic homeostasis during cytokinesis and cell morphogenesis.

As a TRP channel, Pkd2p could potentially regulate the turgor pressure through a number of ways. It may control the ion influx to directly modulate the turgor. As a permissive cation channel, Pkd2p could allow the calcium influx to regulate the turgor pressure, considering its localization on the plasma membrane (Palmer *et al.*, 2005). In this way, Pkd2p may be similar to another TRP channel TRPV4 that regulates osmolarity of animal cells (Colbert *et al.*, 1997; Strotmann *et al.*, 2000; Liedtke and Friedman, 2003). Alternatively, Pkd2p may regulate the intracellular osmolarity indirectly through interacting with the other signaling pathways including the SIN pathway. It is worth noticing that both Pkd2p and the Sid2p/Mob1p complex localize to the cell division plane during late cytokinesis (Sparks *et al.*, 1999; Goss *et al.*, 2014). More studies are needed to

determine how Pkd2p acts through these potential mechanisms to regulate the turgor pressure.

Molecular functions of the Pkd2p family proteins

Our study identified a novel function of the fungal Pkd2p family proteins in regulating cytokinesis. This family of transmembrane proteins can be found among many fung speciies and is one of 17 essential fungal protein families (Hsiang and Baillie, 2005). Four *Saccharomyces cerevisiae* Pkd2 homologues, Flc1 (flavin carrier 1), Flc2, Flc3, and YOR365c, have been identified. Unlike fission yeast *pkd2*, none of these budding yeast homologues is essential (Protchenko *et al.*, 2006; Rigamonti *et al.*, 2015; Vazquez *et al.*, 2016). However, deletion of both *flc1* and *flc2* is lethal. These four proteins appear to play a role in osmotic regulation (Protchenko *et al.*, 2006), heme transportation (Protchenko *et al.*, 2006) and calcium homeostasis (Rigamonti *et al.*, 2015), although the molecular mechanism of their functions is unknown. It also remains to be determined whether any of these four budding yeast genes is required for cytokinesis. Other fungal Pkd2p homologues include *spray* of *Neurospora crassa* (Bok *et al.*, 2001), FlcA/B/C of *Aspergillus fumigatus* (de Castro *et al.*, 2017), and CaFlc1-3 of *Candida albicans* (Protchenko *et al.*, 2006). Interestingly, all of them regulate hyphal growth of the fungi, similar to the fission yeast Pkd2p regulation of cell growth. Our proposed role of Pkd2p in regulating osmotic homeostasis would be consistent with the central role of turgor in the fungal growth (Lew, 2011).

In multicellular eukaryotic organisms, Pkd2p is required for several developmental processes but the underlying molecular mechanism is far from clear. Both *D. melanogaster* and *C. elegans* homologues of Pkd2p contribute to the locomotion of sperms and the *pkd2* mutations lead to male sterility (Barr and Sternberg, 1999; Gao *et al.*, 2003; Watnick *et al.*, 2003). The human Pkd2p homologues PKD1 and PKD2 are required for cardiac development and left-right orientation (Wu *et al.*, 2000; Pennekamp *et al.*, 2002). Their function in the kidney has been studied most extensively, because loss of function mutations of either genes result in a hereditary human disease, ADPKD (for review, see Chapin and Caplan, 2010). This renal disorder affects more than 600,000 Americans alone. It is characterized by progressive proliferation of liquid-filled cysts in the kidney that often culminates to a terminal renal failure (Mochizuki *et al.*, 1996). Despite years of work, it still remains largely unknown how the mutations of these human Pkd2p homologues lead to ADPKD. Study of fission yeast Pkd2p and its function in osmotic homeostasis will likely provide us with critical insights into the molecular functions of human PKD1 and PKD2 as well as the pathogenesis of ADPKD.

MATERIALS AND METHODS

Yeast genetics

Yeast cell culture and genetics procedures were carried out according to the standard methods. A SporePlay+ dissection microscope (Singer, England) was used for tetrad dissections. Most yeast strains were constructed through PCR-based homologous recombination (Bahler *et al.*, 1998). To construct *trp663::trp663-GFP*, *trp1322::trp1322-GFP*, and *pkd2::pkd2-GFP*, we integrated the mEGFP sequence at the endogenous locus of each gene. We constructed *trp1322*$^{+}$/*trp1322*Δ by removing one copy of the open reading frame (ORF). The diploid cells were then sporulated and selected to isolate *trp1322*Δ. The *trp663*Δ mutant is from a fission yeast deletion library (Bioneer, South Korea) and was confirmed by PCR. To examine the viability of the *pkd2*Δ mutant, we constructed the diploid *pkd2*$^{+}$/*pkd2*Δ by deleting one copy of the ORF. The diploid was then sporulated and dissected into more than 20 tetrads that were deposited onto either YE5s or YE5s plus 1.2 M sorbitol agar plates. For microscopy of *pkd2*Δ spores, a small block of agar containing the spore was removed from the agar plate and deposited on a glass-bottomed Petri dish for observation. To replace the endogenous *pkd2* promoter, we integrated inducible *nmt1* promoters at the endogenous locus, preceding the start codon of the *pkd2* ORF. To construct *pkd2::P81nmt1-pkd2-GFP-ura*, we constructed *pkd2::pkd2-GFP-ura* first, before replacing the endogenous promoter with *P81nmt1*. The resulting yeast strains were confirmed by both PCR and the Sanger sequencing method. The *pkd2-81KD* spores were obtained by digesting the tetrads with glusulase II (PerkinElmer) and observed under a YE5s agar pad for 8–12 h with bright-field microscopy.

Microscopy

For microscopy, exponentially growing yeast cells at 25°C with a density between 5.0×10^6/ml and 1.0×10^7/ml in YE5s liquid media (unless specified), were harvested by centrifugation at 4000 rpm for 1 min and resuspended in YE5s. The cells were then applied to a 25% gelatin + YE5s pad and sealed under the coverslip with VALEP (a mix of an equal amount of Vaseline, lanolin, and paraffin). Live microscopy was carried out on an Olympus IX71 microscope equipped with both a 100× (NA = 1.41) and a 60× (NA = 1.40) objective lens, a confocal spinning-disk unit (CSU-X1; Yokogawa, Japan), a motorized XY stage, and a Piezo Z Top plate (ASI). The images were captured on an Ixon-897 EMCCD camera controlled by iQ3.0 (Andor, Ireland). Solid-state lasers of 488 and 561 nm were used in the confocal fluorescence microscopy, at a power of no more than 5 mW (<10%). Unless specified, we imaged cells by acquiring a Z-series of 15 slices at a step size of 0.5 µm. Live microscopy was conducted in a room where the temperature was maintained at around 20°C. To minimize the temperature variations, we usually imaged both wild-type and the *pkd2* mutant cells on the same date. For temperature-sensitive mutants, we inoculated the cultures at the restrictive temperatures for 4 h before either imaging them at room temperature immediately or fixing the cells before imaging. For visualizing the cell wall, we stained cells with 10 µg/ml calcofluor (Sigma) and used an Olympus IX81 microscope equipped with a CCD camera and a mercury lamp for the epifluorescence microscopy. For visualizing the actin cytoskeletal structure, we fixed cells with 16% EM-grade paraformaldehyde (EMS) and stained them with bodipy-phallacidin (Invitrogen), as described previously (Chen *et al.*, 2014).

Electron microscopy

Transmission electron microscopy was carried out at the Microscopy and Image Analysis Laboratory core at the University of Michigan (Ann Arbor, MI). Briefly, exponentially growing cells were harvested and rinsed with 0.1 M phosphate buffer (pH = 7.4) before being fixed with 2.5% glutaraldehyde (EMS). The fixed cells were stained with 1% osmium tetroxide to increase contrast and embedded in epoxy resin overnight at 4°C. The samples were then sectioned at a thickness of 70 nm (Leica EM UC7). The EM specimens were imaged with a JEM-1400 (Joel, Japan) transmission electron microscope. The thickness of the cell wall was measured as the average distance between the plasma membrane and the outer boundary of the cell wall, at more than 10 randomly selected sites.

Image processing

We used ImageJ (National Institutes of Health) to process all the images, with either freely available or customized macros/plug-ins. For quantitative analysis, the fluorescence micrographs were

corrected for X-Y drifting using the StackReg plug-in (Thevenaz *et al.*, 1998) and for photobleaching using the EMBLTools plug-in (Rietdorf, EMBL Heidelberg). Average intensity projections of Z-slices were used for quantifications. The contractile ring localization of Pkd2p-GFP was quantified by measuring the GFP fluorescence in a 3.6 μm × 0.8 μm (36 × 8 pixels) rectangle centering on the cell division plane, corrected with background subtraction through measuring the background fluorescence intensities in two 3.6 μm × 0.2 μm rectangles (36 × 2 pixels) adjoined to the division plane. The cell width was measured using both live and fixed cells, which yielded similar results. The length of cytokinetic cells was measured using bright-field images of the live cells expressing Rlc1p-tdTomato.

The nuclear localization of Sty1p-GFP was measured by quantifying GFP fluorescence intensities in the nuclei with background subtraction. To simplify the analysis, we assumed the nucleus as a circle of 2 μm diameter that centers on the nucleus localization of Sty1p-GFP. The background fluorescence was determined by measuring the fluorescence intensities of Sty1p-GFP in the cytoplasm surrounding the nucleus. The total area of a cell was measured based upon the cytoplasmic fluorescence of Styp1-GFP after the cell was segmented semiautomatically using the Binary conversion and Analysis Particles tools of ImageJ.

The rate of ring closure is measured by analyzing fluorescence kymographs of a ring during cytokinesis. The kymograph was constructed from the time-lapse fluorescence micrographs (Figure 4E), which was then used to determine both the start and end of ring closure. The diameter of a ring was determined at the start of ring closure. For quantitative fluorescence microscopy, our spinning-disk confocal microscope was calibrated using a previously published method (Wu and Pollard, 2005). Briefly, we imaged wild-type and seven fission yeast strains expressing GFP-tagged proteins to produce a calibration curve ($R^2 > 0.95$). Slope of the calibration curve was used to determine the ratio of fluorescence intensities to molecule numbers. The figures were made with Canvas X (ACDsee systems, Canada). The domain structure of Pkd2p is based on the prediction by Pfam and the National Center for Biotechnology Information (NCBI). The predicted topology of Pkd2p was created by Protter (http://wlab.ethz.ch/protter/), a protein topology data aggregation server (Omasits *et al.*, 2014).

ACKNOWLEDGMENTS

This work was supported by the University of Toledo Start-up Fund and deArce-Koch Memorial Endowment Fund to Q.C. We thank the groups of Carlos R. Vázquez de Aldana (IBFG, Spain), Juan Carlos Ribas (University of Salamanca, Spain), Dannel McCollum (University of Massachusetts Medical School), and Jianqiu Wu (Ohio State University) for generously sharing yeast strains with us. We express our appreciation of the help from our colleagues at the Department of Biological Sciences, Richard Komuniecki and Song-Tao Liu, in the preparation of the manuscript.

REFERENCES

Abenza JF, Couturier E, Dodgson J, Dickmann J, Chessel A, Dumais J, Carazo Salas RE (2015). Wall mechanics and exocytosis define the shape of growth domains in fission yeast. Nat Commun 6, 8400.

Arasada R, Pollard TD (2014). Contractile ring stability in *S. pombe* depends on F-BAR protein Cdc15p and Bgs1p transport from the Golgi complex. Cell Rep 8, 1533–1544.

Arnadottir J, Chalfie M (2010). Eukaryotic mechanosensitive channels. Annu Rev Biophys 39, 111–137.

Atilgan E, Magidson V, Khodjakov A, Chang F (2015). Morphogenesis of the fission yeast cell through cell wall expansion. Curr Biol 25, 2150–2157.

Aydar E, Palmer CP (2009). Polycystic kidney disease channel and synaptotagmin homologues play roles in *Schizosaccharomyces pombe* cell wall synthesis/repair and membrane protein trafficking. J Membr Biol 229, 141–152.

Bahler J, Wu JQ, Longtine MS, Shah NG, McKenzie A 3rd, Steever AB, Wach A, Philippsen P, Pringle JR (1998). Heterologous modules for efficient and versatile PCR-based gene targeting in *Schizosaccharomyces pombe*. Yeast 14, 943–951.

Balasubramanian MK, McCollum D, Chang L, Wong KC, Naqvi NI, He X, Sazer S, Gould KL (1998). Isolation and characterization of new fission yeast cytokinesis mutants. Genetics 149, 1265–1275.

Barr MM, DeModena J, Braun D, Nguyen CQ, Hall DH, Sternberg PW (2001). The *Caenorhabditis elegans* autosomal dominant polycystic kidney disease gene homologs lov-1 and pkd-2 act in the same pathway. Curr Biol 11, 1341–1346.

Barr MM, Sternberg PW (1999). A polycystic kidney-disease gene homologue required for male mating behaviour in *C. elegans*. Nature 401, 386–389.

Basi G, Schmid E, Maundrell K (1993). TATA box mutations in the *Schizosaccharomyces pombe* nmt1 promoter affect transcription efficiency but not the transcription start point or thiamine repressibility. Gene 123, 131–136.

Bok JW, Sone T, Silverman-Gavrila LB, Lew RR, Bowring FJ, Catcheside DE, Griffiths AJ (2001). Structure and function analysis of the calcium-related gene spray in *Neurospora crassa*. Fungal Genet Biol 32, 145–158.

Chan CM, Chen Y, Hung TS, Miller AL, Shipley AM, Webb SE (2015). Inhibition of SOCE disrupts cytokinesis in zebrafish embryos via inhibition of cleavage furrow deepening. Int J Dev Biol 59, 289–301.

Chang F, Drubin D, Nurse P (1997). cdc12p, a protein required for cytokinesis in fission yeast, is a component of the cell division ring and interacts with profilin. J Cell Biol 137, 169–182.

Chapin HC, Caplan MJ (2010). The cell biology of polycystic kidney disease. J Cell Biol 191, 701–710.

Chen Q, Courtemanche N, Pollard TD (2014). Aip1 promotes actin filament severing by cofilin and regulates the constriction of the cytokinetic contractile ring. J Biol Chem 290, 2289–2300.

Chen Q, Pollard TD (2011). Actin filament severing by cofilin is more important for assembly than constriction of the cytokinetic contractile ring. J Cell Biol 195, 485–498.

Chen Q, Pollard TD (2013). Actin filament severing by cofilin dismantles actin patches and produces mother filaments for new patches. Curr Biol 23, 1154–1162.

Christensen AP, Corey DP (2007). TRP channels in mechanosensation: direct or indirect activation? Nat Rev Neurosci 8, 510–521.

Colbert HA, Smith TL, Bargmann CI (1997). OSM-9, a novel protein with structural similarity to channels, is required for olfaction, mechanosensation, and olfactory adaptation in *Caenorhabditis elegans*. J Neurosci 17, 8259–8269.

Cortes JC, Ishiguro J, Duran A, Ribas JC (2002). Localization of the (1,3)β-D-glucan synthase catalytic subunit homologue Bgs1p/Cps1p from fission yeast suggests that it is involved in septation, polarized growth, mating, spore wall formation and spore germination. J Cell Sci 115, 4081–4096.

Cortes JC, Konomi M, Martins IM, Munoz J, Moreno MB, Osumi M, Duran A, Ribas JC (2007). The (1,3)β-D-glucan synthase subunit Bgs1p is responsible for the fission yeast primary septum formation. Mol Microbiol 65, 201–217.

Cortes JC, Sato M, Munoz J, Moreno MB, Clemente-Ramos JA, Ramos M, Okada H, Osumi M, Duran A, Ribas JC (2012). Fission yeast Ags1 confers the essential septum strength needed for safe gradual cell abscission. J Cell Biol 198, 637–656.

Coste B, Mathur J, Schmidt M, Earley TJ, Ranade S, Petrus MJ, Dubin AE, Patapoutian A (2010). Piezo1 and Piezo2 are essential components of distinct mechanically activated cation channels. Science 330, 55–60.

Coue M, Brenner SL, Spector I, Korn ED (1987). Inhibition of actin polymerization by latrunculin A. FEBS Lett 213, 316–318.

Courtemanche N, Pollard TD, Chen Q (2016). Avoiding artefacts when counting polymerized actin in live cells with LifeAct fused to fluorescent proteins. Nat Cell Biol 18, 676–683.

Davi V, Tanimoto H, Ershov D, Haupt A, De Belly H, Le Borgne R, Couturier E, Boudaoud A, Minc N (2018). Mechanosensation dynamically coordinates polar growth and cell wall assembly to promote cell survival. Dev Cell 45, 170–182 e177.

Davidson R, Pontasch JA, Wu JQ (2016). Sbg1 is a novel regulator for the localization of the β-glucan synthase Bgs1 in fission yeast. PLoS One 11, e0167043.

de Castro PA, Chiaratto J, Morais ER, Dos Reis TF, Mitchell TK, Brown NA, Goldman GH (2017). The putative flavin carrier family FlcA-C is important for *Aspergillus fumigatus* virulence. Virulence 8, 797–809.
Degols G, Shiozaki K, Russell P (1996). Activation and regulation of the Spc1 stress-activated protein kinase in *Schizosaccharomyces pombe*. Mol Cell Biol 16, 2870–2877.
Dekker N, Speijer D, Grun CH, van den Berg M, de Haan A, Hochstenbach F (2004). Role of the α-glucanase Agn1p in fission-yeast cell separation. Mol Biol Cell 15, 3903–3914.
De Lozanne A, Spudich JA (1987). Disruption of the Dictyostelium myosin heavy chain gene by homologous recombination. Science 236, 1086–1091.
Effler JC, Kee YS, Berk JM, Tran MN, Iglesias PA, Robinson DN (2006). Mitosis-specific mechanosensing and contractile-protein redistribution control cell shape. Curr Biol 16, 1962–1967.
Eng K, Naqvi NI, Wong KC, Balasubramanian MK (1998). Rng2p, a protein required for cytokinesis in fission yeast, is a component of the actomyosin ring and the spindle pole body. Curr Biol 8, 611–621.
Fankhauser C, Reymond A, Cerutti L, Utzig S, Hofmann K, Simanis V (1995). The *S. pombe* cdc15 gene is a key element in the reorganization of F-actin at mitosis. Cell 82, 435–444.
Gao Z, Ruden DM, Lu X (2003). PKD2 cation channel is required for directional sperm movement and male fertility. Curr Biol 13, 2175–2178.
Garcia Cortes JC, Ramos M, Osumi M, Perez P, Ribas JC (2016). The cell biology of fission yeast septation. Microbiol Mol Biol Rev 80, 779–791.
Gonzalez-Perrett S, Kim K, Ibarra C, Damiano AE, Zotta E, Batelli M, Harris PC, Reisin IL, Arnaout MA, Cantiello HF (2001). Polycystin-2, the protein mutated in autosomal dominant polycystic kidney disease (ADPKD), is a Ca^{2+}-permeable nonselective cation channel. Proc Natl Acad Sci USA 98, 1182–1187.
Goss JW, Kim S, Bledsoe H, Pollard TD (2014). Characterization of the roles of Blt1p in fission yeast cytokinesis. Mol Biol Cell 25, 1946–1957.
Hanaoka K, Qian F, Boletta A, Bhunia AK, Piontek K, Tsiokas L, Sukhatme VP, Guggino WB, Germino GG (2000). Co-assembly of polycystin-1 and -2 produces unique cation-permeable currents. Nature 408, 990–994.
Hergovich A, Hemmings BA (2012). Hippo signalling in the G2/M cell cycle phase: lessons learned from the yeast MEN and SIN pathways. Semin Cell Dev Biol 23, 794–802.
Hou MC, Salek J, McCollum D (2000). Mob1p interacts with the Sid2p kinase and is required for cytokinesis in fission yeast. Curr Biol 10, 619–622.
Hsiang T, Baillie DL (2005). Comparison of the yeast proteome to other fungal genomes to find core fungal genes. J Mol Evol 60, 475–483.
Hughes J, Ward CJ, Peral B, Aspinwall R, Clark K, San Millan JL, Gamble V, Harris PC (1995). The polycystic kidney disease 1 (PKD1) gene encodes a novel protein with multiple cell recognition domains. Nat Genet 10, 151–160.
Johnson AE, McCollum D, Gould KL (2012). Polar opposites: Fine-tuning cytokinesis through SIN asymmetry. Cytoskeleton (Hoboken) 69, 686–699.
Kitayama C, Sugimoto A, Yamamoto M (1997). Type II myosin heavy chain encoded by the myo2 gene composes the contractile ring during cytokinesis in *Schizosaccharomyces pombe*. J Cell Biol 137, 1309–1319.
Krapp A, Gulli M, Simanis V (2004). SIN and the art of splitting the fission yeast cell. Curr Biol 14, R722–R730.
Kung C (2005). A possible unifying principle for mechanosensation. Nature 436, 647–654.
Laplante C, Berro J, Karatekin E, Hernandez-Leyva A, Lee R, Pollard TD (2015). Three myosins contribute uniquely to the assembly and constriction of the fission yeast cytokinetic contractile ring. Curr Biol 25, 1955–1965.
Le Goff X, Woollard A, Simanis V (1999). Analysis of the cps1 gene provides evidence for a septation checkpoint in *Schizosaccharomyces pombe*. Mol Gen Genet 262, 163–172.
Lew RR (2011). How does a hypha grow? The biophysics of pressurized growth in fungi. Nat Rev Microbiol 9, 509–518.
Liedtke W, Friedman JM (2003). Abnormal osmotic regulation in trpv4–/– mice. Proc Natl Acad Sci USA 100, 13698–13703.
Liu J, Wang H, McCollum D, Balasubramanian MK (1999). Drc1p/Cps1p, a 1,3-β-glucan synthase subunit, is essential for division septum assembly in *Schizosaccharomyces pombe*. Genetics 153, 1193–1203.
Ma Y, Sugiura R, Koike A, Ebina H, Sio SO, Kuno T (2011). Transient receptor potential (TRP) and Cch1-Yam8 channels play key roles in the regulation of cytoplasmic Ca^{2+} in fission yeast. PLoS One 6, e22421.
Martinac B, Buechner M, Delcour AH, Adler J, Kung C (1987). Pressure-sensitive ion channel in *Escherichia coli*. Proc Natl Acad Sci USA 84, 2297–2301.
Martin-Cuadrado AB, Duenas E, Sipiczki M, Vazquez de Aldana CR, del Rey F (2003). The endo-β-1,3-glucanase eng1p is required for dissolution of the primary septum during cell separation in *Schizosaccharomyces pombe*. J Cell Sci 116, 1689–1698.
Maundrell K (1990). nmt1 of fission yeast. A highly transcribed gene completely repressed by thiamine. J Biol Chem 265, 10857–10864.
McCollum D, Gould KL (2001). Timing is everything: regulation of mitotic exit and cytokinesis by the MEN and SIN. Trends Cell Biol 11, 89–95.
Millar JB, Buck V, Wilkinson MG (1995). Pyp1 and Pyp2 PTPases dephosphorylate an osmosensing MAP kinase controlling cell size at division in fission yeast. Genes Dev 9, 2117–2130.
Mishra M, Kashiwazaki J, Takagi T, Srinivasan R, Huang Y, Balasubramanian MK, Mabuchi I (2013). In vitro contraction of cytokinetic ring depends on myosin II but not on actin dynamics. Nat Cell Biol 15, 853–859.
Misumi Y, Miki K, Takatsuki A, Tamura G, Ikehara Y (1986). Novel blockade by brefeldin A of intracellular transport of secretory proteins in cultured rat hepatocytes. J Biol Chem 261, 11398–11403.
Mochizuki T, Wu G, Hayashi T, Xenophontos SL, Veldhuisen B, Saris JJ, Reynolds DM, Cai Y, Gabow PA, Pierides A, *et al*. (1996). PKD2, a gene for polycystic kidney disease that encodes an integral membrane protein. Science 272, 1339–1342.
Munoz J, Cortes JC, Sipiczki M, Ramos M, Clemente-Ramos JA, Moreno MB, Martins IM, Perez P, Ribas JC (2013). Extracellular cell wall β(1,3) glucan is required to couple septation to actomyosin ring contraction. J Cell Biol 203, 265–282.
Nauli SM, Alenghat FJ, Luo Y, Williams E, Vassilev P, Li X, Elia AE, Lu W, Brown EM, Quinn SJ, *et al*. (2003). Polycystins 1 and 2 mediate mechanosensation in the primary cilium of kidney cells. Nat Genet 33, 129–137.
Omasits U, Ahrens CH, Muller S, Wollscheid B (2014). Protter: interactive protein feature visualization and integration with experimental proteomic data. Bioinformatics 30, 884–886.
Palmer CP, Aydar E, Djamgoz MB (2005). A microbial TRP-like polycystic-kidney-disease-related ion channel gene. Biochem J 387, 211–219.
Palmer CP, Zhou XL, Lin J, Loukin SH, Kung C, Saimi Y (2001). A TRP homolog in *Saccharomyces cerevisiae* forms an intracellular Ca^{2+}-permeable channel in the yeast vacuolar membrane. Proc Natl Acad Sci USA 98, 7801–7805.
Pazour GJ, San Agustin JT, Follit JA, Rosenbaum JL, Witman GB (2002). Polycystin-2 localizes to kidney cilia and the ciliary level is elevated in orpk mice with polycystic kidney disease. Curr Biol 12, R378–R380.
Pennekamp P, Karcher C, Fischer A, Schweickert A, Skryabin B, Horst J, Blum M, Dworniczak B (2002). The ion channel polycystin-2 is required for left-right axis determination in mice. Curr Biol 12, 938–943.
Pinheiro D, Hannezo E, Herszterg S, Bosveld F, Gaugue I, Balakireva M, Wang Z, Cristo I, Rigaud SU, Markova O, *et al*. (2017). Transmission of cytokinesis forces via E-cadherin dilution and actomyosin flows. Nature 545, 103–107.
Pollard TD (2010). Mechanics of cytokinesis in eukaryotes. Curr Opin Cell Biol 22, 50–56.
Pollard TD, Wu JQ (2010). Understanding cytokinesis: lessons from fission yeast. Nat Rev 11, 149–155.
Proctor SA, Minc N, Boudaoud A, Chang F (2012). Contributions of turgor pressure, the contractile ring, and septum assembly to forces in cytokinesis in fission yeast. Curr Biol 22, 1601–1608.
Protchenko O, Rodriguez-Suarez R, Androphy R, Bussey H, Philpott CC (2006). A screen for genes of heme uptake identifies the FLC family required for import of FAD into the endoplasmic reticulum. J Biol Chem 281, 21445–21457.
Ranade SS, Syeda R, Patapoutian A (2015). Mechanically activated ion channels. Neuron 87, 1162–1179.
Rappaport R (1967). Cell division: direct measurement of maximum tension exerted by furrow of echinoderm eggs. Science 156, 1241–1243.
Rigamonti M, Groppi S, Belotti F, Ambrosini R, Filippi G, Martegani E, Tisi R (2015). Hypotonic stress-induced calcium signaling in *Saccharomyces cerevisiae* involves TRP-like transporters on the endoplasmic reticulum membrane. Cell Calcium 57, 57–68.
Robertson AM, Hagan IM (2008). Stress-regulated kinase pathways in the recovery of tip growth and microtubule dynamics following osmotic stress in *S. pombe*. J Cell Sci 121, 4055–4068.

Rundle DR, Gorbsky G, Tsiokas L (2004). PKD2 interacts and co-localizes with mDia1 to mitotic spindles of dividing cells: role of mDia1 IN PKD2 localization to mitotic spindles. J Biol Chem 279, 29728–29739.
Salimova E, Sohrmann M, Fournier N, Simanis V (2000). The *S. pombe* orthologue of the *S. cerevisiae* mob1 gene is essential and functions in signalling the onset of septum formation. J Cell Sci 113 (Pt 10), 1695–1704.
Sanger JM, Sanger JW (1980). Banding and polarity of actin filaments in interphase and cleaving cells. J Cell Biol 86, 568–575.
Sawin KE, Snaith HA (2004). Role of microtubules and tea1p in establishment and maintenance of fission yeast cell polarity. J Cell Sci 117, 689–700.
Sethi K, Palani S, Cortes JC, Sato M, Sevugan M, Ramos M, Vijaykumar S, Osumi M, Naqvi NI, Ribas JC, *et al.* (2016). A new membrane protein Sbg1 links the contractile ring apparatus and septum synthesis machinery in fission yeast. PLoS Genet 12, e1006383.
Shiozaki K, Russell P (1995). Cell-cycle control linked to extracellular environment by MAP kinase pathway in fission yeast. Nature 378, 739–743.
Sipiczki M (2007). Splitting of the fission yeast septum. FEMS Yeast Res 7, 761–770.
Sparks CA, Morphew M, McCollum D (1999). Sid2p, a spindle pole body kinase that regulates the onset of cytokinesis. J Cell Biol 146, 777–790.
Srivastava V, Iglesias PA, Robinson DN (2016). Cytokinesis: robust cell shape regulation. Semin Cell Dev Biol 53, 39–44.
Stachowiak MR, Laplante C, Chin HF, Guirao B, Karatekin E, Pollard TD, O'Shaughnessy B (2014). Mechanism of cytokinetic contractile ring constriction in fission yeast. Dev Cell 29, 547–561.
Straight AF, Cheung A, Limouze J, Chen I, Westwood NJ, Sellers JR, Mitchison TJ (2003). Dissecting temporal and spatial control of cytokinesis with a myosin II Inhibitor. Science 299, 1743–1747.
Strotmann R, Harteneck C, Nunnenmacher K, Schultz G, Plant TD (2000). OTRPC4, a nonselective cation channel that confers sensitivity to extracellular osmolarity. Nat Cell Biol 2, 695–702.
Sukharev SI, Blount P, Martinac B, Blattner FR, Kung C (1994). A large-conductance mechanosensitive channel in *E. coli* encoded by mscL alone. Nature 368, 265–268.
Sukharev SI, Blount P, Martinac B, Guy HR, Kung C (1996). MscL: a mechanosensitive channel in *Escherichia coli.* Soc Gen Physiol Ser 51, 133–141.
Thevenaz P, Ruttimann UE, Unser M (1998). A pyramid approach to subpixel registration based on intensity. IEEE Trans Image Process 7, 27–41.
Thiyagarajan S, Munteanu EL, Arasada R, Pollard TD, O'Shaughnessy B (2015). The fission yeast cytokinetic contractile ring regulates septum shape and closure. J Cell Sci 128, 3672–3681.
Vazquez HM, Vionnet C, Roubaty C, Mallela SK, Schneiter R, Conzelmann A (2016). Chemogenetic E-MAP in *Saccharomyces cerevisiae* for identification of membrane transporters operating lipid flip flop. PLoS Genet 12, e1006160.
Walker RG, Willingham AT, Zuker CS (2000). A *Drosophila* mechanosensory transduction channel. Science 287, 2229–2234.
Watnick TJ, Jin Y, Matunis E, Kernan MJ, Montell C (2003). A flagellar polycystin-2 homolog required for male fertility in *Drosophila*. Curr Biol 13, 2179–2184.
Wu JQ, Kuhn JR, Kovar DR, Pollard TD (2003). Spatial and temporal pathway for assembly and constriction of the contractile ring in fission yeast cytokinesis. Dev Cell 5, 723–734.
Wu G, Markowitz GS, Li L, D'Agati VD, Factor SM, Geng L, Tibara S, Tuchman J, Cai Y, Park JH, *et al*. (2000). Cardiac defects and renal failure in mice with targeted mutations in Pkd2. Nat Genet 24, 75–78.
Wu JQ, Pollard TD (2005). Counting cytokinesis proteins globally and locally in fission yeast. Science 310, 310–314.
Wu LJ, Sweet TB, Clapham DE (2010). International Union of Basic and Clinical Pharmacology. LXXVI. Current progress in the mammalian TRP ion channel family. Pharmacol Rev 62, 381–404.
Yoder BK, Hou X, Guay-Woodford LM (2002). The polycystic kidney disease proteins, polycystin-1, polycystin-2, polaris, and cystin, are co-localized in renal cilia. J Am Soc Nephrol 13, 2508–2516.
Zhou Z, Munteanu EL, He J, Ursell T, Bathe M, Huang KC, Chang F (2015). The contractile ring coordinates curvature-dependent septum assembly during fission yeast cytokinesis. Mol Biol Cell 26, 78–90.